PHYSICAL REVIEW B VOLUME 27, NUMBER 3 1 FEBRUARY 1983

Electron holography and magnetic specimens

Akira Fukuhara, Kohsei Shinagawa, Akira Tonomura, and Hideo Fujiwara
Central Research Laboratory, Hitachi Ltd., Kokubunji, Tokyo 185, Japan
(Received 5 May 1982; revised manuscript received 12 August 1982)

Electron holography and electron interferometry for magnetic specimens have no close analogy to counterparts in visible-ray optics, while there are such counterparts for nonmagnetic specimens. Formulas are presented for the relation between the magnetic structure of specimens and the phase information that can be determined using such techniques. Some simulation examples using the formulas are demonstrated including a display of the Aharonov-Bohm effect in a form of interferometry. In addition, how a magnetic monopole should appear on an electron hologram and how its strength and sign should be determined from the hologram are illustrated. The interference fringes on the hologram must look like "a dislocation in a set of parallel lines." The number of extra lines corresponds to the strength of the monopole.

I. INTRODUCTION

While interference of electron waves associated with diffraction phenomena has long been observed, almost conventionally, with diffraction apparatuses or electron microscopes, that of the "off-axis" type, i.e., interference between electron waves propagated in two separate directions, has been technologically difficult to observe in practice. Recently, however, better spatial coherency has been realized through development of electron sources of the field-emission type.[1] As a result, off-axis electron holography[2] has now reached a new, practical stage.

The phase information in an electron wave transmitted through a specimen can be visualized by means of optical image reconstruction and optical interferometry with electron holograms. Phase changes in the wave during transmission through a specimen are classified into those of electric or magnetic origin. The former, for example, the effect of electrostatic inner potential within the specimen has the closest analogy with refraction effect in the visible-ray optics; however, the phase change due to magnetism has no analogy outside of charged-particle optics, so its interpretation may be more difficult in some cases.

Nevertheless, "magnetic" phase changes give us information related to magnetic structure. Therefore, properly designed electron holography can provide a unique method of observing magnetic specimens which are beyond the capability of other methods for their size or thickness. Furthermore, it is expected that this technique will complement Lorentz microscopy,[3] a conventional method making use of the effect of Lorentz force on defocused images in electron microscopy.

The purposes of this paper are, first, to clarify the relation between the magnetization within specimens and the resulting electron phase, second, to illustrate several simulations, including a display of the Aharonov-Bohm effect from an interferogram, and, finally, to describe how a magnetic monopole should appear in a similar interferogram.

II. MAGNETIC PHASE

Let us suppose a plane wave of electrons is being propagated onto a plane of observation. The phase distribution on this plane changes when a magnetic specimen is set in the middle of the path. This change is recorded on a hologram by making the wave (object wave) interfere with another wave (reference wave) split from the same source by a biprism and propagated in a different direction. This is the well-known principle of holography and can now be realized in a properly equipped electron microscope. Reconstruction of the object wave in optical form is performed by illuminating such a hologram, or strictly speaking a magnified hologram, with the coherent wave from a laser.

The phase of the object electron wave is also reproduced and can be visualized by means of the interference between this wave and another optical wave (comparison wave). Visualization is in the form of a set of equal-phase lines, i.e., a contour map of the "phase changes" when the comparison wave is adjusted to be the same as the object wave for an empty specimen. When the comparison wave is tilted we have an interferogram consisting of fringes. This is the experimental situation that has been attained so far. Although the interferogram is another contour map corresponding to a tilted level

 ©1983 The American Physical Society

of the phase change, we will discriminate in this paper between contour maps and interferograms in the above sense for clarity.

Deflection of an electron beam is so small in experiments with a thin magnetic specimen in an electron microscope operated at conventional voltages (50–200 kV) that the estimate of magnetic phase change $\Delta\Phi$ in the WKB approximation is sufficiently accurate:

$$\Delta\Phi_L=(2\pi e/h)\int_L \vec{A}\cdot\vec{ds}\ , \tag{1}$$

where the integral is taken along a straight line L corresponding to the classical electron trajectory, e and h are the electron charge and Planck constant, respectively, and $\vec{A}$ is the vector potential originating from the magnetic specimen. Arbitrariness in $\vec{A}$ within the Coulomb gauge is assumed to be eliminated here as

$$\text{div}\ A=0\ , \tag{2}$$

and $A=0$ at infinity from the specimen. The quantity $\Delta\Phi_L$ is the two-dimensional distribution of the magnetic phase on a plane (observation plane) perpendicular to the electron path. The integration on the right-hand side of Eq. (1) will be carried out over $(-\infty,+\infty)$ along L. This is justified provided that the value of $\vec{A}$ vanishes, in effect, on the plane where the reference beam is superposed.

The difference of the phase change between two classical trajectories, L_1 and L_2, can be expressed by Stokes's theorem as

$$\Delta\Phi_{L_1}-\Delta\Phi_{L_2}=(2\pi e/h)\int_{S_{12}} B_n dS\ . \tag{3}$$

Since B_n is the component of magnetic-flux density $\vec{B}$ normal to surface S_{12} enclosed by L_1 and L_2, the integral stands for the magnetic flux passing through S_{12}. This simple expression shows that the lines on the phase-contour map are parallel to the flux density integrated along L and projected onto a plane perpendicular to L and that two adjacent lines enclose a magnetic-flux quantum, h/e $(=4.1\times10^{-15}$ Wb), irrespective of the electron energy.

The vector potential $\vec{A}(P)$ at point P is expressed in terms of the magnetization $\vec{M}(Q)$ at Q in the specimen and the vacuum permeability μ_0:

$$\vec{A}(P)=[\mu_0/(4\pi)]\int dV_Q[\vec{M}(Q)\times\vec{R}_{PQ}]/(R_{PQ})^3\ , \tag{4}$$

provided that the region where $\vec{M}$ is not zero does not extend to infinity. $\vec{R}_{PQ}$ is a distance vector from P to Q (Fig. 1). After integration along L in Eq. (1) we have

$$\Delta\Phi(p)=(\mu_0 e/h)\int dV_Q[\vec{M}(Q)\times\vec{r}_{pq}]_L/(r_{pq})^2\ , \tag{5}$$

where p and q are, respectively, projections of P and Q onto a plane perpendicular to L, $\vec{r}_{pq}$ is the distance vector from p to q, and subscript L means the component parallel to L. Starting with Eq. (5) we can obtain different expressions of $\Delta\Phi(p)$ under particular assumptions about $\vec{M}$, or for convenience in numerical estimation.

In an actual experiment the specimen may be composed of domains in such a way that the magnetization is not continuous across boundaries but is differentiable within each domain. In such a case

$$\Delta\Phi(p)=(\mu_0 e/h)\sum\left[\oint dS_Q[\vec{n}\times\vec{M}(Q)]_L \ln r_{pq} + \int dV_Q[\vec{\nabla}\times\vec{M}]_L \ln r_{pq}\right]\ , \tag{6}$$

where the summation is over all domains, and $\vec{n}$ is the outward normal to each domain surface.

Magnetic closure structures provide special conditions. For example, if $\vec{M}$ is mathematically divergence free and its normal component is continuous across boundaries including the outer surface, $\vec{B}$ equals $\mu_0\vec{M}$ inside and vanishes outside of the specimen so that

$$\vec{\nabla}^{(2)}[\Delta\Phi(p)]=(\mu_0 e/h)\int_L[\vec{M}\times\vec{ds}]_L\ . \tag{7}$$

The integral here is along the trajectory line L passing through point p, and $\vec{\nabla}^{(2)}$ is the two-dimensional gradient operator. In this particular case we can read magnetization distribution more directly from the contour map. The photograph shown by Fig. 3(b) in Ref. 2 roughly corresponds to such a case.

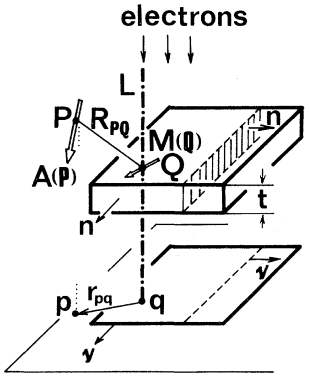

FIG. 1. Geometric relations among electron trajectory L, the specimen, and its projection.

III. SIMULATIONS OF PHASE-CONTOUR MAPS

If the specimen has a constant thickness t and $\vec{M}$ can be assumed to be independent of the coordinate parallel to L, then the contributions from the top and bottom faces of the specimen are canceled out and

$$\Delta\Phi(p)=(\mu_0 e/h)\sum\left\{\oint dl_q[\vec{v}\times\vec{M}(q)]_L \ln r_{pq} + \int dv_q[\vec{\nabla}^{(2)}\times\vec{M}(q)]_L \times\ln r_{pq}\right\}. \quad (8)$$

The first integral is along the outline of each projected domain with the outward normal $\vec{v}$ and the second one is over the projected domain. Equation (8) can be used for numerical simulations of phase-contour maps from presumed flux distributions. A few simulation examples using Eq. (8) are illustrated here in Fig. 2.

Discussions so far have assumed $\vec{M}$ to simulate the phase distributions for comparison with experimental data. One may be tempted to reverse the procedure, i.e., to derive magnetization distributions of modest accuracy from experimental phase contours. However, this is not possible. As is proved by a standard technique of vector analysis, the gradient field for any potential function which is zero on the specimen surface can be added to $\vec{M}$ without resulting in any change in $\Delta\Phi$. This means that there can be no unique $\vec{M}$ distribution for a given $\Delta\Phi$. Clearly we need more information than $\Delta\Phi$ distributions to restrict and eventually determine $\vec{M}$ distributions.

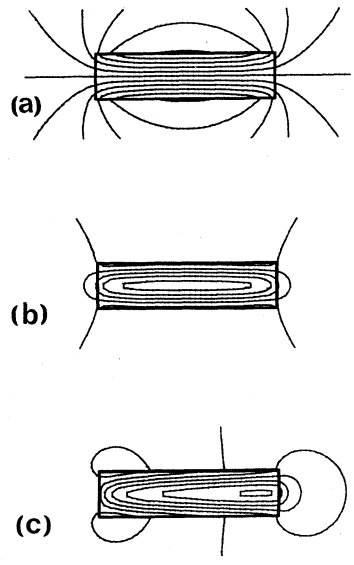

FIG. 2. Simulated phase-contour maps. All sample sizes: 1 μm$\times$4 μm$\times$50 nm; saturated magnetization: 1 T/μ_0. $\vec{M}$ is parallel to the longer edge except in the domain-wall regions. The wall, 0.5-μm wide, is along the longer center line of each rectangle. (a) Rectangular single domain. (b) Rectangle with a Bloch wall. (c) Rectangle with a Néel wall. Direction of $\vec{M}$ in the wall rotates counterclockwise within the paper plane from top to bottom.

Another simulated example is shown here concerning a demonstration of the Aharonov-Bohm effect. In quantum mechanics the wave function of a charged particle is affected by a magnetic vector potential in an observable way even where no magnetic flux exists. This Aharonov-Bohm effect[4] reveals itself as a difference in phase between two waves after having traveled in different directions around a magnetic sample leaking no magnetic flux. Pioneering experiments on this effect have been published by several authors,[5] including the work by Mollenstedt *et al.* with tiny solenoids. However, some people still doubt its existence or the validity of the experiments.[6] Discussions of works purporting to show its nonexistence are not convincing to the authors of the present paper.

The holographic method of phase measurement described in previous sections can be applied to confirm the Aharonov-Bohm effect in a new way. Let us suppose a ferromagnetic sample is in a doubly connected or toroidal form with a magnetic closure structure such that there is no magnetic-flux leakage, as is shown schematically in Fig. 3(a). Greenberger[12] has suggested the usage of such a ferromagnetic doughnut and Kuper[13] has proposed the idea of flux confinement by a hollow superconductive torus.

An electron hologram taken of such a specimen is set in an optical reconstruction system and the ob-

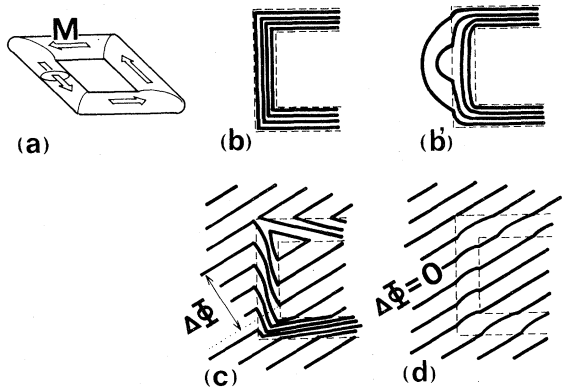

FIG. 3. Holographic display of Aharonov-Bohm effect. (a) Doubly connected shape with a magnetic closure structure. (b) Phase-contour map without flux leakage. (b') Phase-contour map with flux leakage. (c) Interferogram showing Aharonov-Bohm effect. (d) Interferogram for null magnetization but only refraction effect.

ject wave field is optically reproduced. This wave field is overlapped with a parallel comparison wave and then a tilted comparison wave, and the resulting interference patterns just on the image plane of the object wave are observed as a contour map and an interferogram, respectively. These patterns will appear schematically like Figs. 3(b) and 3(c).

Since the interference is observed on the image plane, the outline of the toroid must be seen superposed on the pattern so that each location on the pattern corresponds to a partial object wave having passed a particular part of the object plane within the resolution accuracy. We can measure, by tracing or counting the fringes as shown in Fig. 3(c), the phase difference $\Delta\Phi$ between the two waves, each of which has been propagated through outer or inner space around the toroid magnet but has never passed the magnetic flux inside it. When the magnetization and the thickness of the toroid are estimated beforehand, we can check whether the dependence of the phase difference on these values is consistent with Eq. (7). When sample preparation does not form a complete closure structure, flux leakage will result. This can also be recognized on a contour map, as shown in Fig. 3(b'), and evaluated in order to decide if it will seriously affect the conclusion or not. Experimental work was done by the same group in parallel with this paper and its result was reported separately.[7]

Furthermore, if the specimen temperature can be raised above the Curie point in the recording apparatus, another interferogram like Fig. 3(d) can be obtained. This combined with one below the Curie point, will quite convincingly show the Aharonov-Bohm effect.

IV. HOW A MAGNETIC MONOPOLE LOOKS IN A HOLOGRAM

Magnetic monopoles have been widely researched in both artificial production and exploration in nature since Dirac's hypothetical proposition[8] about their existence and quantization of their strength g. It was reported quite recently that a moving monopole was recorded by using a superconductive detector.[9]

The sign and the strength of a monopole can be determined also from a hologram provided that it is stably fixed on a proper substrate as an electron-microscope specimen. The hologram is formed in the same way as in our previous example.

While the magnetic flux around a monopole is unique, the singularity of corresponding vector potential $\vec{A}$ can never be restricted only to the monopole location. Thus difficulty arises in defining the phase factor of the electron wave function propagated around it. Wu and Yang[10] suggested the following.

The whole space except the monopole point is divided into two partially overlapping regions, in each of which $\vec{A}$ is defined to be regular in form. In the overlap of the two regions the two discrete forms of $\vec{A}$ are related by a gauge transformation, which creates multipling phase factor S between the two corresponding wave functions.

One possible choice given by Wu and Yang is

$$
\begin{aligned}
&R_a:\ 0\le\theta<\pi/2+\delta,\ 0<r,\ A_\phi=\frac{g}{4\pi r\sin\theta}(1-\cos\theta),\ A_r=A_\theta=0\ ,\\
&R_b:\ \pi/2-\delta<\theta\le\pi,\ 0<r,\ A_\phi=\frac{-g}{4\pi r\sin\theta}(1+\cos\theta),\ A_r=A_\theta=0\ ,\\
&S=S_{ba}=\exp(-ige\phi/h)\ .
\end{aligned}
\tag{9}
$$

Since S should be single valued, we obtain Dirac's quantization

$$ge/h=D\ , \tag{10}$$

an integer. The above result, (9), is applied to derive the phase relation between the objective and reference electron wave and, eventually, to give the intensity distribution in the hologram. A schematic arrangement for hologram recording is illustrated in Fig. 4(a). It should be noted that the wave function of the reference wave continues from region R_a to region R_b at $\phi=0$. Assuming that the object beam is vertically incident to the recording plane and that the amplitudes of both waves are equal, we obtain

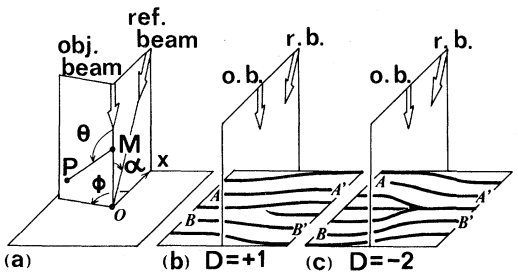

FIG. 4. Holographic observation of a magnetic monopole. (a) Arrangement for hologram recording. M is a monopole and $P(r,\theta,\phi)$ is the point for estimating vector potential $\vec{A}$. (b) Hologram for $D=+1$. D is an integer defining the monopole strength. (c) Hologram for $D=-2$.

the intensity I of interference pattern in terms of x and ϕ,

$$I(x,\phi)=1+\cos(kx\sin\alpha-D\phi+\delta_0)\ , \qquad (11)$$

where k is the wave number of electrons and δ_0 is a constant corresponding to the optical-path difference between the two waves.

Since the WKB approximation is adopted here again, this expression is not correct in the vicinity of the exact shadow point of the monopole. However, it is accurate enough for the following conclusion. Examples of the interference patterns are shown in Figs. 4(b) and 4(c). The patterns look like crystal-lattice planes around and edge dislocation and thus one can count the number of extra lattice planes and decide on which side they extend. It should be remembered that such a dislocationlike pattern should never appear for any divergence-free flux field.

More precisely, any pair of dark lines [A-A' and B-B' in Figs. 2(b) and 4(c)] enclosing the projection of the monopole confines a different number of dark lines between them on opposite sides of the projection. Subtraction of the number on the right from that on the left gives integer D, provided that right or left is viewed from the direction of the tilted reference beam. This determination of D is independent of δ_0, although δ_0 does affect the entire pattern especially near the shadow point of the monopole. Finally, it should be noted that Dirac's quantization condition (10) for g is indispensable to defining any hologram pattern.

V. CONCLUDING REMARKS

It has been derived that a two-dimensional vector distribution of magnetic flux integrated and projected along the incident electron trajectory is what we observe as a contour map or equal-phase fringes produced from the electron hologram of a magnetic specimen. This should be the basis of interpretation when the technique is applied to investigation of magnetic materials.[11] The phase increment attributed to magnetism is also expressed as an integral of the magnetic vector potential along the trajectory, in a fairly good approximation. This phase has no counterpart in visible-ray optics.

When the sample has a magnetic closure structure in a doubly connected shape, there is a space free of magnetic flux with a nonvanishing vector potential around the sample.[12,13] This type of sample, combined with the holographic phase determination of electron waves, provides a clear-cut test of the Aharonov-Bohm effect as was shown in a recent experimental work.[7]

It has also been shown that a magnetic monopole appears as a particular pattern, similar to "a dislocation in a set of parallel lines" on a hologram. No magnetic-flux distribution can produce this type of pattern as long as the distribution is divergence free. Thus electron-holographic interferometry affords a decisive method of recognizing a monopole, provided that it can be fixed properly as a sample.

ACKNOWLEDGMENTS

We gratefully acknowledge the kind comments of Professor C. N. Yang, State University of New York, Stony Brook, who gave us his considered opinion about this work on his visit to our laboratory.

[1]A. Tonomura, T. Matsuda, J. Endo, H. Todokoro, and T. Komoda, J. Electron Microsc. 28, 1 (1979).
[2]A. Tonomura, T. Matsuda, J. Endo, T. Arii, and K. Mihama, Phys. Rev. Lett. 44, 1430 (1980).
[3]M. S. Cohen, J. Appl. Phys. 38, 4966 (1967).
[4]Y. Aharonov and D. Bohm, Phys. Rev. 115, 485 (1959).
[5]R. G. Chambers, Phys. Rev. Lett. 5, 3 (1960); H. A. Fowler, L. Marton, J. A. Simpson, and J. A. Suddeth, J. Appl. Phys. 32, 1153 (1961); H. Boersch, H. Hamisch, K. Grohmann, and D. Wohlleben, Z. Phys. 165, 79 (1961); G. Mollenstedt and W. Bayh, Phys. Bl. 18, 299 (1962).
[6]D. S. DeWitt, Phys. Rev. 125, 2189 (1962); P. Bocchieri and A. Loinger, Nuovo Cimento 47, 475 (1978); 51A-56A, 55 (1980); Lett. Nuovo Cimento 25, 476 (1979); S. M. Roy, Phys. Rev. Lett. 44, 111 (1980).
[7]A. Tonomura, T. Matsuda, R. Suzuki, A. Fukuhara, N. Osakabe, H. Umezaki, J. Endo, K. Shinagawa, Y. Sugita, and H. Fujiwara, Phys. Rev. Lett. 48, 1443 (1982).
[8]P. A. M. Dirac, Proc. R. Soc. London, Ser. A 133, 60 (1931).
[9]B. Cabrera, Phys. Rev. Lett. 48, 1378 (1982).
[10]T. T. Wu and C. N. Yang, Phys. Rev. D 12, 3845 (1975).
[11]The technique has been actually applied to observe micromagnetic structures in thin films of Permalloy and nickel: A. Tonomura, T. Matsuda, H. Tanabe, N. Osakabe, J. Endo, A. Fukuhara, K. Shinagawa, and H. Fujiwara, Phys. Rev. B 25, 6799 (1982).
[12]D. M. Greenberger, Phys. Rev. D 23, 1460 (1981).
[13]C. G. Kuper, Phys. Lett. 79A, 413 (1980).